On the instability characteristics of a reattaching shear layer with nonlaminar separation

M. A. Z. Hasan and A. S. Khan
Mechanical Engineering Department, King Fahd University of Petroleum and Minerals, Dhahran, Saudi Arabia

The instability characteristics of a reattaching shear layer with nonlaminar separation were investigated via controlled excitation. The most dominant structure of the flow, termed the *step mode* of instability, was at $St_h = 0.185$, which was independent of the separating boundary layer's state. An explanation has been provided for whether the spectral energy for an excited flow will be concentrated at the excitation frequency f or at its higher harmonic component $2f$. The shear layer with transitional separation failed to support the growth of a disturbance. This was attributed to the high level of turbulence intensity in the initial boundary layer. The downstream evolution of longitudinal velocity spectra showed that the step-mode instability peak quickly takes over the shear-layer instability peak at $St_\theta \cong 0.011$ for the turbulent-separation case and prevails further downstream of the reattachment point.

Keywords: free shear layer; shear-layer instability; large-scale structure; initial condition; reattaching shear layer; separation; step mode of instability

Introduction

Flow with shear-layer separation and reattachment occurs in many practical engineering devices. Of the various flow geometries with reattaching shear layers, the backward-facing step flow has received most of the attention from various investigators for two reasons. First, the separation point in a backward-facing step geometry is very clearly defined, and second, it has been selected as one of the two central test cases for comparison with numerical prediction methods (Kline et al., 1982). The basic flow over a backward-facing step has been treated by many researchers (Chandrsuda and Bradshaw 1981; Moss and Baker 1980; Etheridge and Kemp 1978; Eaton and Johnston 1980; and others).

Since the discovery of the presence of large-scale coherent structures in two-dimensional (2-D) plane mixing layers (Brown and Roshko 1974; Winant and Browand 1974), the role of these structures in the development of free shear layers has been investigated extensively. The same is not true for the large-eddy structure in reattaching shear layers. One of the first studies concentrating on the large-eddy structure in a reattaching shear layer was by McGuinness (1978). Later, Troutt et al. (1984) studied the dynamics of the coherent vortical structures that develop and evolve in a backward-facing step flow. In recent times, external forcing, at discrete frequencies, has been applied at the separation point of a backward-facing step to study the instability characteristics, as well as the effect of forcing on the large-scale structures.

Address reprint requests to Dr. Hasan at Mechanical Engineering Department, King Fahd University of Petroleum and Minerals, Dhahran 31261, Saudi Arabia.

Received 6 August 1991; accepted 24 February 1992

Bhattacharjee et al. (1986) showed that the most effective forcing Strouhal number, St_h, was in the range of 0.2 to 0.4, and this was nearly constant over a broad range of step Reynolds numbers Re_h covering transitional and turbulent separation boundary layers. Roos and Kegelman (1986), on the other hand, showed that the natural instability frequency for a backward-facing step flow was at $St_h \cong 0.4$, and the effect of forcing on the reattachment length was minimal for the transitional separation boundary layer. The reduced effectiveness of shear-layer excitation in the transition range was attributed to the fact that a single-frequency excitation failed to couple equally well with both laminar and turbulent layers. In our opinion, this explanation is probably tentative and needs further study. Roos and Kegelman (1986) also observed, for turbulent separation, maximum concentration of energy at the first harmonic ($2f$) of the excitation frequency f, rather than at f itself. No explanation was provided for this behavior other than attributing it to the complexities of the reattaching shear layer due to external excitation.

In a recent study of backward-facing step flow with laminar separation (Hasan 1992), it has been shown that the reattaching shear layer supports two distinct modes of instabilities, i.e., the *shear-layer mode* of instability at $St_\theta \cong 0.012$ corresponding to the natural roll-up frequency of the shear layer and the *step mode* of instability at $St_h \cong 0.185$. The step mode is equivalent to the well-known *preferred mode* of the plane or axisymmetric shear layers (Hussain and Zaman 1981).

While recent studies (Bhattacharjee et al. 1986; Roos and Kegelman 1986; Hasan 1992) have shed new light on the large-scale structures in reattaching shear layers and their modification under excitation, our understanding of the instability characteristics of a reattaching shear layer, especially for nonlaminar separation, is far from complete.

The objectives of this study were to investigate the instability characteristics of a reattaching shear layer and the modification

of the large-scale structures under controlled excitation for nonlaminar separations (i.e., transitional and turbulent). It was decided to investigate the cause of the insensitivity of a reattaching shear layer with transitional separation to external excitation. Understanding of the large-scale structure dynamics and their modification under various initial conditions will lead to a better design of engineering devices with reattaching shear layers.

Experimental facilities and procedures

The experiments were carried out in the wind tunnel at King Fahd University of Petroleum and Minerals (KFUPM), with a test section of length 3 m having a cross-section of 1.1 m × 0.8 m. Downstream of the blower exit, a large divergent–convergent section, with a number of screens and a honeycomb, was used to ensure high-quality uniform flow in the test section. The tunnel was run with a variable speed DC motor, and the velocity range available was 2.5 to 25 m/s. The freestream turbulence level was 0.1% of U_∞ for $U_\infty = 5.5$ m/s.

A backward-facing step was installed in the test section. The step height h was 3 cm. The schematic of the test setup is given in Figure 1a. All working surfaces were constructed from smooth laminated wood. The downstream length of the bottom plate from the separation point was 100 cm. Along the centerline of the bottom plate, 2-mm diameter holes were drilled 2 cm apart to measure the surface static pressure distribution with plastic tubes connected to a manometer. Two-dimensionality of the flow was checked by measuring the longitudinal mean and fluctuating velocity profiles at four spanwise locations for both $x/h = 2$ and $x/h = 13$ (see below).

The acoustic excitation technique used in this study was similar to the ones used by Hasan (1983) and Kibens (1980) to study the axisymmetric jet flow structure. The flow excitation was introduced through a narrow slit of 1-mm width at the separation edge. The details of the separation point are shown in Figure 1b.

The 20-mm × 20-mm cavity in the aluminium section was connected to four copper tubes of 10-mm diameter. The ends of the copper tubes were connected to the speaker box with 12-mm tygon tubes of equal length. The equal length of the tubes ensured excitation at the separation point to be at the same phase across the whole width of the plate. The variation of the excitation level was less than 5% in the spanwise direction

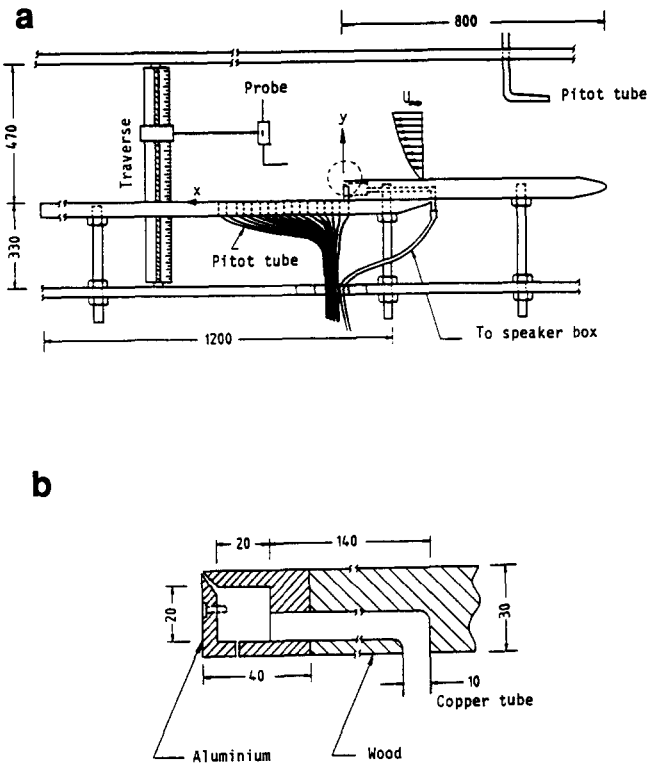

Figure 1 Schematic of backward-facing step and excitation device. (a) Details of the step; (b) enlarged cross-sectional view of the excitation device. All dimensions are in mm

over four step heights. A 30-cm-diameter loudspeaker (150 watts) was driven by a signal generator and an audio amplifier to introduce the excitation at desired frequencies and amplitudes.

Excitation at a discrete frequency, f, enables one to track the downstream growth of the disturbance wave at f via the increased organization of the flow as compared to the unexcited flow. The excitation level at the separation point (i.e., $x = 0$) was kept at 2.8 ± 0.2% of U_∞ at the $y_{0.95}$ (where $U/U_\infty = 0.95$) location, and was continuously monitored with a fixed reference probe. The measurement probe was controlled via a

Notation

f	Frequency
h	Step height
H	Shape factor (δ^*/θ)
Re_h ($\equiv U_\infty h/\nu$)	Reynolds number based on h
St_h ($\equiv fh/U_\infty$)	Strouhal number based on h
St_θ ($\equiv f\theta/U_\infty$)	Strouhal number based on θ
u	Longitudinal fluctuation intensity
$\bar{u}^2$	Normal Reynolds stress in x-direction
u_f	Wave amplitude at frequency f
u_{2f}	Wave amplitude at the first harmonic of f
u_{ex}	Longitudinal fluctuation intensity due to excitation
u_τ	Friction velocity in the boundary layer
$u(t)$	Instantaneous longitudinal velocity
U	Longitudinal mean velocity
U_∞	Freestream mean velocity
U^+	U/u_τ
x	Downstream direction
y	Transverse direction
y^+	yu_τ/ν
y_n	Transverse location where $U/U_\infty = n$
z	Spanwise direction

Greek symbols

δ	Boundary-layer thickness
δ^*	Displacement thickness
θ	Momentum thickness
ν	Kinematic viscosity

three-dimensional (3-D) computer-controlled traverse system with a resolution of 0.06 mm.

The acoustic mode of the tunnel was investigated as part of a different project (Prof. M. U. Budair, private communication). The dominant acoustic mode was found to be around 300 Hz. The frequencies of interest in this study were much lower than 300 Hz. Also, it should be noted that the acoustic mode was picked up by hot-wire only when the flow impinged on a sharp edge. The detailed study of the shear-layer response to the acoustic excitation by Hasan (1992) showed no dominant spectral peak associated with the tunnel mode. It is our belief that the interaction between the acoustic modes of the wind tunnel and the shear layer, if any, is minimal.

All the velocity data were measured with a DISA 55 M01 standard hot-wire anemometer system. The anemometer was operated in the constant temperature mode with 50% overheat ratio. The hot-wire signal was linearized. The data were recorded in a four-channel B & K 7033 tape recorder for later analysis. Spectral analysis of the velocity signal was performed with a B & K 2033 high-resolution spectrum analyzer with 400 lines and a selectable frequency range. Each spectrum represents the average of 64 spectra. The static pressure measurements were carried out with TEM manometers (model 5585) with an accuracy of 0.01 mb. The reattachment length was checked by surface-oil flow visualization.

Flow in a reattaching shear layer is complicated by the presence of recirculation and a high level of turbulence intensity. These factors impose some restrictions on the accuracy of conventional hot-wire measurements. Hot-wire results are likely to be reliable only if the ratio u/U (u and U being local longitudinal turbulence intensity and mean velocity, respectively), is, say, less than about 0.30 (Chandrusuda and Bradshaw 1981). For flow over a normal plate, Castro and Haque (1987) and Jaroch and Fernholz (1989) showed that in the reattachment region, x-wire probes undermeasured the Reynolds stresses compared to pulsed-wire measurement. The comparison of pulsed-wire and single hot-wire measurements in a backward-facing step flow by Eaton and Johnston (1980) showed good agreement between the two measurement techniques in the region of peak turbulence intensity, i.e., near the center of the shear layer. They estimated that the single hot-wire measurements of $\bar{u}^2$ are expected to be lower than those taken with a pulsed wire, although probably by 1 or 2%. It will be seen that the data presented here provide considerable useful qualitative information to enhance our understanding of reattaching flow.

Results and discussion

Since the initial boundary-layer state plays an important role in the development of a reattaching shear layer (Roos and Kegelman 1986), documentation of the separation boundary layers was considered essential. Attempts were made to generate both transitional and turbulent boundary-layer states, for the same Re_h value, by using different trips. However, this proved unsuccessful because the separation boundary layer was not fully turbulent for $U_\infty \leqslant 10$ m/s even with trips. After detailed investigation of the separation boundary layer with different combinations of U_∞ and trips, the final U_∞ values selected for transitional and turbulent separation boundary layers were 7.5 and 15 m/s, respectively. The corresponding Re_h values were 1.5×10^4 and 3.0×10^4. A nylon chord of 2-mm diameter placed 20 mm upstream of the separation edge was used as the trip. Details of the boundary-layer measurements are given in the following section.

Initial conditions

The U/U_∞ and u/U_∞ profiles at the separation point for $U_\infty = 7.5$ m/s and 15 m/s are shown in Figure 2a. Unless otherwise specified, lines joining the data points in the figures in this article are for clarity. Among other measures that characterize the initial condition, only U/U_∞ and u/U_∞ profiles have been used as the identifiers of the initial condition. The characteristic length scales of the initial boundary layer, viz., the boundary-layer thickness, δ, the displacement thickness, δ^*, and momentum thickness, θ, as well as the shape factor, H, for the two cases are listed in Table 1.

For $U_\infty = 15$ m/s, the separation boundary layer was turbulent, as suggested by the $u(t)$ signal, U/U_∞ and u/U_∞ profiles, and the corresponding shape factor. This was further checked by plotting the U/U_∞ profile for the turbulent case in wall coordinates U^+ and y^+ (Figure 2b), and thus enabling comparison with the equilibrium flat-plate turbulent boundary layer. The friction velocity u_τ, was determined from the mean velocity data by the cross-plot (Clauser-plot) technique. The data in Figure 2b follow closely the universal logarithmic curve $U^+ = 5.61 \log y^+ + 5.2$, with a value of $u_\tau = 0.81$ m/s giving the best fit. The very weak wake region is probably due to the

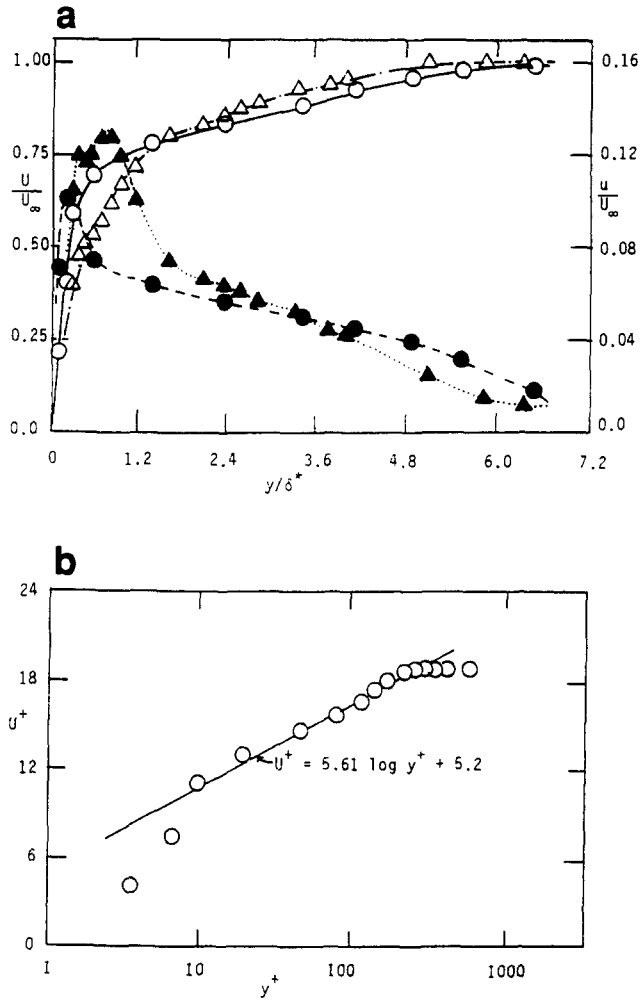

Figure 2 (a) Boundary-layer profiles of U/U_∞ (open) and u/U_∞ (solid) at the separation point. Symbols: ○, turbulent separation ($Re_h = 30{,}000$); △, transitional separation ($Re_h = 15{,}000$). (b) U/U_∞ data of Figure 2a for the turbulent separation case in U^+ *versus* y^+ coordinates

Table 1 Boundary-layer parameters

Boundary-layer state	U_∞ (m/s)	Re_h	Re_θ	δ (mm)	δ^* (mm)	θ (mm)	$H = \frac{\delta^*}{\theta}$
Transitional	7.5	1.5×10^4	865	14.6	2.996	1.73	1.73
Turbulent	15.0	3.0×10^4	904	8.44	1.327	0.906	1.47

trip used for making the boundary layer turbulent. Many studies have shown that a boundary layer takes a much longer distance than the 20 mm used in this study for the flow to recover from the disturbance caused by the trip. Another factor contributing to the weak wake region is perhaps the favorable pressure gradient present close to the separation point. Troutt et al. (1984) observed a similar weak wake region for their study. The shape factor for the U/U_∞ profile at $U_\infty = 7.5$ m/s is 1.73, which is between the expected values of 1.4 and 2.6 for turbulent and laminar boundary layers, respectively. Thus, this case has been classified as transitional.

As the boundary layer changes from laminar to transitional, a sharp peak in the u/U_∞ profile develops close to the wall, unlike the broad peak for the laminar boundary layer (Hasan 1992). For a laminar boundary layer, u/U_∞ represents potential flow fluctuation. The u/U_∞ peak is also present for the turbulent case. The peak amplitudes of u/U_∞ in the boundary layer for laminar, turbulent, and transitional separations are 0.012, 0.104, and 0.130, respectively.

The effect of excitation on boundary-layer parameters was minimal (Hasan 1992), and, thus, was not considered here.

Two-dimensionality of the flow

Two-dimensionality of the flow was checked for $Re_h = 3 \times 10^4$ by measuring U/U_∞ and u/U_∞ profiles at four spanwise (z/h) locations for $x/h = 2$ (Figure 3a) and $x/h = 13$ (Figure 3b). The complete profiles were measured on one side of the centerline, while some spot checks were made on the other side. The U/U_∞ and u/U_∞ profiles spanning $z/h = 0$ to ± 1 show excellent collapse at both $x/h = 2$ and $x/h = 13$. While it is recognized that $z/h = +1$ is a restricted spanwise range for the two-dimensionality check, data beyond this range were difficult to measure due to the positioning problem of the traverse system inside the test section. But surface-oil flow visualization used to identify the reattachment point revealed the reattachment line to be 2-D over $z/h = +4$. This confirms the two-dimensionality of the flow along the midspan of the entire measurement region.

Downstream evolution of the wave amplitude

The instability characteristics of a shear layer can be described by the downstream growth of a disturbance wave in the shear layer. The downstream variation of the wave amplitude (u_f) for various excitation frequencies is shown in Figure 4a for the turbulent separation case. The data were measured at the cross-stream location of maximum longitudinal fluctuation intensity. The wave amplitudes, in general, grow in the downstream direction and reach a peak by $x/h = 2$. It is clear from Figure 4a that an initially turbulent shear layer can support the growth of a disturbance, but unlike a laminar shear layer, the initial growth is highly nonlinear, and this is to be expected. The downstream growth rate of u_f data in Figure 4a was found to be qualitatively similar to the theoretically predicted growth rate of a nonlinear instability wave in a free shear layer (Goldstein and Hultgren 1988). Note that the peak

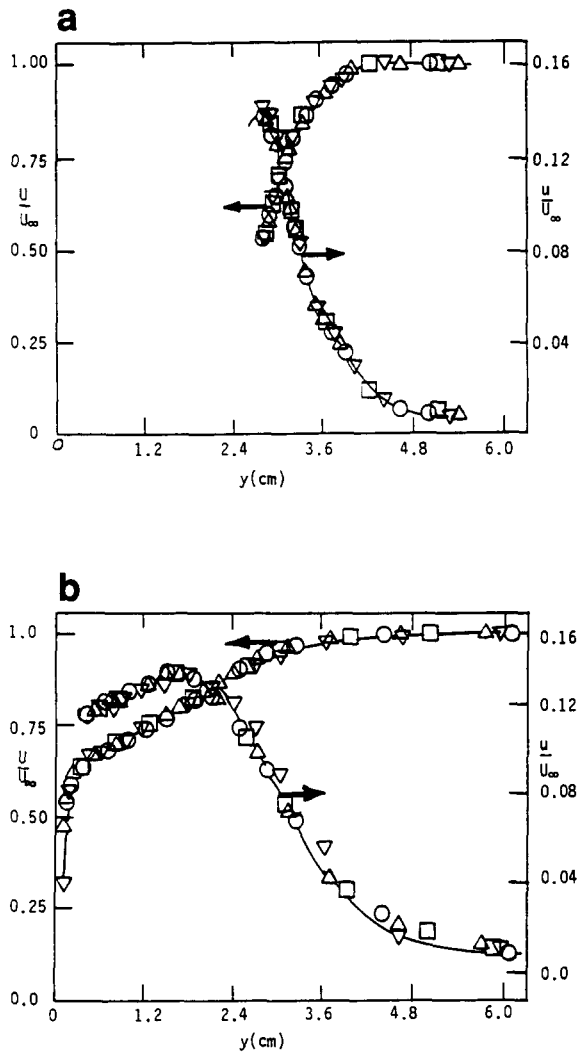

Figure 3 U/U_∞ and u/U_∞ profiles at different z/h locations for the turbulent separation ($Re_h = 30{,}000$) at (a) $x/h = 2$; (b) $x/h = 13$. Symbols for the z/h values are as follows: ○, 0.0; △, 0.33; □, 0.67; ▽, 1

value of u_f has a maximum for $St_h = 0.185$ and occurs at $x/h \cong 2$ (or $x/\theta \cong 60$).

For $St_h = 0.25$ ($St_\theta \cong 0.008$), the peak value of u_f is about 8 dB lower than that for $St_h = 0.185$. With further increases in St_h, the peak value of u_f again increases and reaches a maximum at $x/\theta \cong 20$ for $St_h = 0.35$ ($St_\theta \cong 0.011$). The shear-layer instability frequency for both free shear flows (Zaman and Hussain 1980; Hussain and Hussain 1983) and reattaching flows (Hasan 1992) with laminar separation has been found to be at $St_\theta \cong 0.012$. We believe that the peak at $St_\theta \cong 0.011$ in Figure 4a is associated with the natural instability of the shear

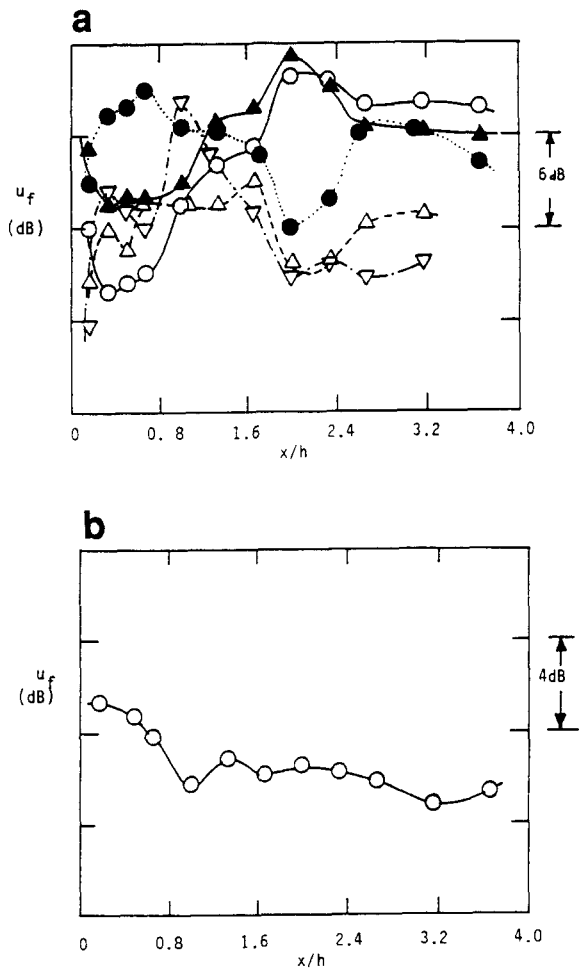

Figure 4 (a) Downstream variation of u_f for the turbulent separation ($Re_h = 30{,}000$). Symbols for the St_θ and St_h values, respectively, are as follows: ○, 0.003, 0.1; ▲, 0.0057, 0.185; △, 0.0075, 0.25; ▽, 0.0087, 0.288; and ●, 0.0105, 0.35. The vertical scale is arbitrary. (b) Downstream variation of u_f for the transitional separation ($Re_h = 15{,}000$) for $St_\theta \cong 0.021$ and $St_h = 0.37$. The vertical scale is arbitrary

layer. It will be shown later that the excitation at $St_\theta \cong 0.011$ organizes the flow dramatically at the excitation frequency.

The u-spectra used to measure u_f values did not show any clear peak at the subharmonic frequency of excitation, which suggests the absence of a regular vortex-merging process, unlike the laminar-separation case (Hasan 1992) where more than one stage of vortex pairing was observed.

In an effort to address the ineffectiveness of a shear layer to external excitation with transitional separation, we briefly digress here to show how a disturbance evolves in a shear layer with transitional separation. Figure 4b shows the downstream variation of u_f for a representative case for $Re_h = 1.5 \times 10^4$ (i.e., with transitional separation). Similar data for other excitation frequencies are given elsewhere (Khan 1990). Note that a shear layer with transitional separation cannot support the growth of a disturbance. This will explain the reduced effectiveness of shear-layer excitation in the transition region observed by Roos and Kegelman (1986). Also, the reduced level of turbulence intensity in the unperturbed flow field with transitional separation (Roos and Kegelman 1986; Khan 1990) can be attributed to the fact that the large-scale structures cannot grow in the shear layer with transitional separation.

We believe that the high level of turbulence intensity in the separation boundary layer for the transitional-separation case prevents the growth of the instability wave. An excitation level higher than the peak turbulence-intensity level of the separation boundary layer may support the growth of the instability wave. This conclusion is drawn based on the successful organization of the *whistler nozzle* flow (Hussain and Hasan 1983) with transitional separation, where a high level of excitation amplitude was available via the resonance of the flow. The present excitation technique cannot deliver a high level of perturbation.

We now return to Figure 4a. Based on the maximum amplitude of u_f, one may conclude that the most dominant structure of the reattaching shear layer with turbulent separation is at $St_h = 0.185$. In order to verify this claim, further measurements were undertaken.

Longitudinal fluctuation intensity variation with f

The relative increase in overall longitudinal fluctuation intensity (u_{ex}/u) as a function of excitation frequency f is shown in Figures 5a and 5b for turbulent and transitional separations, respectively. The data were measured at $x/h = 1$ and at the outer edge of the shear layer, i.e., at the $y_{0.9}$ location.

Note that the maximum relative increase in turbulence

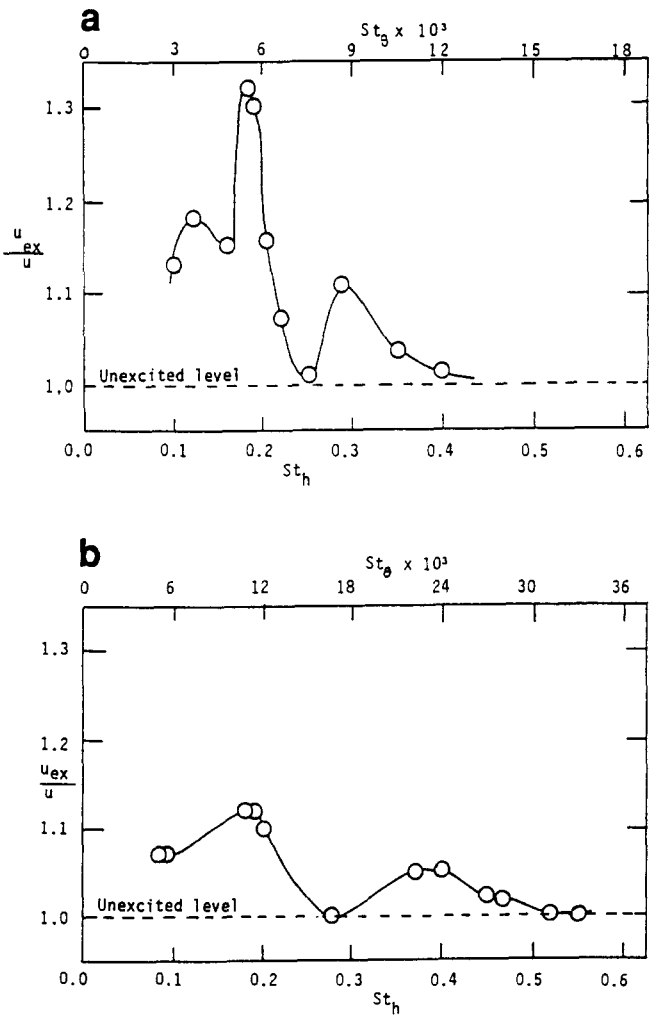

Figure 5 u_{ex}/u *versus* St_h (and St_θ) at $x/h = 1$ and $y_{0.9}$ location for (a) $Re_h = 30{,}000$ (turbulent separation) and (b) $Re_h = 15{,}000$ (transitional separation)

intensity for turbulent separation is about 35% compared to 12% for transitional separation. The maximum increase in turbulence intensity for both turbulent and transitional cases takes place for excitation at $St_h \cong 0.185$, similar to that for laminar separation (Hasan 1992). Unlike the data in Figure 4a, the longitudinal fluctuation intensity levels at $St_h \cong 0.185$ in Figures 5a and 5b are clearly higher than those at other Strouhal numbers. This gives further credence to the fact that $St_h = 0.185$ is the most dominant structure of a reattaching shear layer, which is independent of the separation boundary-layer state.

Based on Figures 4a and 5a, one can argue that the peak u_f occurs when St_θ is half the shear-layer instability frequency. But this is not true either for the laminar case (Hasan 1992) or for the transitional case (Figure 5b), whereas $St_h = 0.185$ is the dominant frequency for all three cases of separation. Note that the other peaks in Figures 5a and 5b are located at multiples or submultiples of $St_\theta \cong 0.006$, indicating some coupling between the step mode and the natural instability of the shear layer. More research with higher St_θ values at other Reynolds numbers than those covered in the present study will be necessary to establish the exact nature of this coupling mechanism.

While data in Figures 4 and 5 shed new light on the instability characteristics of a reattaching shear layer with nonlaminar separation, they provide very little information on the concentration of more energy at the first higher harmonic than at the excitation frequency itself. The response of the velocity spectra to different excitation frequencies at a particular downstream location should be indicative in this regard.

Effect of excitation on longitudinal velocity spectra

The u-spectra with excitation for turbulent separation, i.e., $Re_h = 3 \times 10^4$, are shown in Figure 6. The spectra were measured at $x/h = 1$ and at the transverse location where longitudinal turbulence intensity was the maximum. Also, in Figure 6b, the spectrum for the unexcited flow is shown by the dotted line.

Unlike the laminar-separation case (Hasan 1992) and the data of Bhattacharjee et al. (1986), the unexcited spectrum in Figure 6b shows no clear peak at the natural instability frequency. The absence of a clear spectral peak for the unexcited flow is due to the randomness present for a turbulent separation boundary layer. It is possible that the initial boundary layer of Bhattacharjee et al. (1986) was not fully turbulent. Also, note that excitation primarily increases the energy levels at the excitation frequency f and its higher harmonics and fails to increase the broadband turbulence level.

The baselines for each of the spectra in Figure 6 are separated by an amount corresponding to the excitation frequency f. The origin from where a fan of constant f lines (i.e., f, $2f$, $3f$, etc.) is drawn is at $f = 0$. Under this arrangement, each fan line intersects the baselines at locations proportional to the multiples of f. The vertical lines from the bottom x-axis represent $St_h = 0.185$ and its multiples, while the vertical lines from the top x-axis represent $St_\theta = 0.011$ and its multiples.

For excitation frequency $f = 50$ Hz (Figure 6a), four clear peaks at f, $2f$, $3f$, and $4f$ are visible. The $2f$ component with corresponding St_θ and St_h values of 0.006 and 0.2, respectively, has the maximum amplitude. Concentration of maximum energy at the $2f$ component is also true for excitation at $f = 92.5$ Hz ($St_\theta = 0.0057$, $St_h = 0.185$) in Figure 6b. Roos and Kegelman (1986) also found that initial energy concentration in the shear layer did not occur at the excitation frequency, but at the first harmonic when the separation boundary layer was turbulent. They did not provide any explanation for this

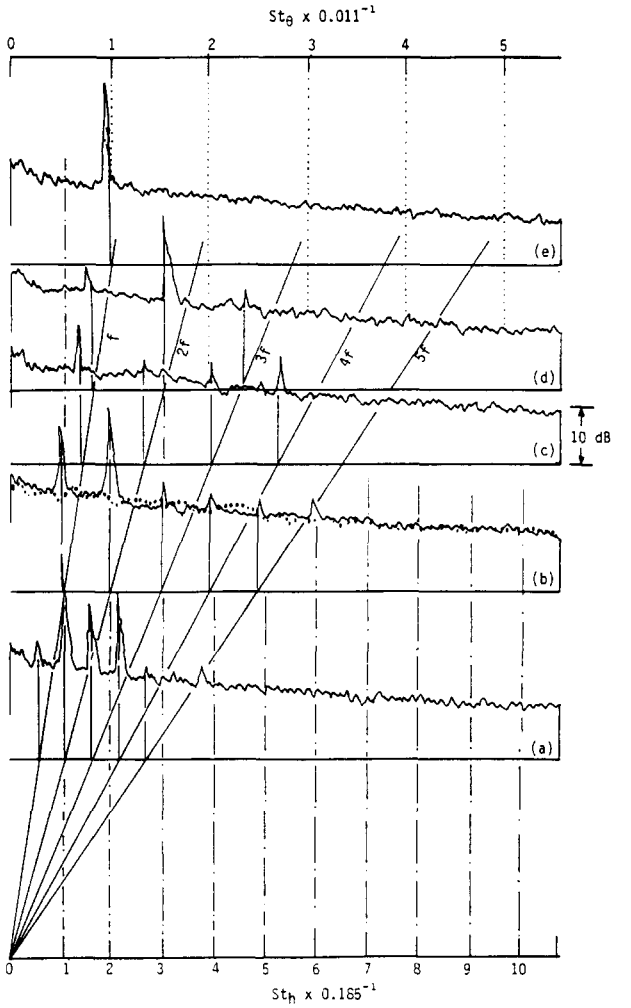

Figure 6 u-spectra for excited flow at $x/h = 1$ and y location corresponding to the maximum u for the turbulent-separation case ($Re_h = 30{,}000$). The dotted line in (b) represents the unexcited spectrum. The excitation frequency f and corresponding St_θ and St_h values, respectively, are (a) 50, 0.003, 0.10; (b) 93.5, 0.0057, 0.185; (c) 125, 0.0075, 0.25; (d) 143.75, 0.0087, 0.288; and (e) 175, 0.0105, 0.35

behavior. The phenomenon of energy concentration at the first harmonic component of the excitation frequency rather than at the excitation frequency itself it not always valid, as indicated in Figures 6c and 6e. When the flow is excited at $St_\theta \cong 0.011$ (Figure 6e), all the energy is concentrated in a single peak at the excitation frequency. As mentioned earlier, $St_\theta \cong 0.011$ is the natural instability frequency of the shear layer, which, for unexcited flow, is masked by the broadband turbulence and the randomness of the flow. However, a slight excitation at this frequency dramatically organizes the flow at the excitation frequency. From Figure 6 it is clear that the maximum energy concentration at $2f$ takes place only when the St_h value due to $2f$ is a multiple of 0.185, i.e., the step mode of instability. Note that in Figures 6a, 6b, and 6d, the $2f$ fan line and one of the multiples of $St_h = 0.185$ intersect the baseline at the same point. This is not the case for Figures 6c and 6e.

Downstream evolution of the u-spectra

The downstream evolution of longitudinal fluctuation velocity spectra measured along the $y_{0.95}$ location for the turbulent separation case is shown in Figure 7. The flow was excited at

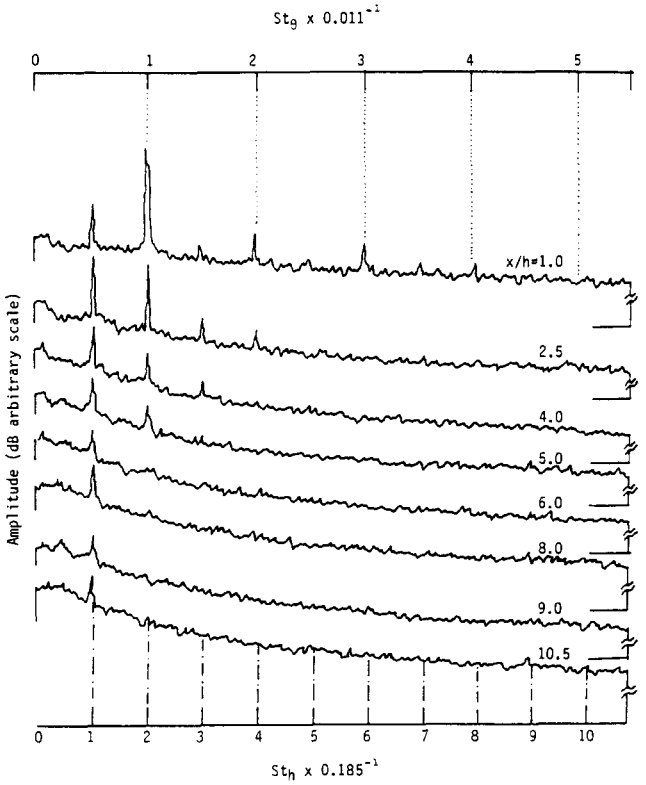

Figure 7 Downstream evolution of u-spectra for excitation at $St_h = 0.185$ for the turbulent separation ($Re_h = 30{,}000$) along the $y_{0.95}$ location

$St_h = 0.185$. Note that at $x/h = 1$, the peak at the excitation frequency f ($f = 92.5$ Hz) is lower than the peak at the first harmonic $2f$.

In Figure 7, the $2f$ peak at $x/h = 1$ corresponds to $St_\theta \cong 0.011$, which we suggest to be the natural instability frequency of the shear layer. At $x/h = 2.5$, the peak at f overtakes the peak at $2f$, and remains stronger than the $2f$ peak further downstream. In fact, the $2f$ component disappears for $x/h \geqslant 6$, which is the postreattachment region. The natural instability frequency of the shear layer is quickly overshadowed by the dominant large-scale structures of the shear layer at $St_h = 0.185$, which persist further downstream of the reattachment point.

The presence of the clear spectral peak at $x/h = 10.5$ strongly indicates the presence of highly organized large-scale structures in the postreattachment region, unlike the flow with laminar separation (Hasan 1992), where no spectral peak was observed for $x/h > 4$. In the case of laminar flow, the absence of a clear spectral peak does not imply the absence of large-scale structures for $x/h > 4$. Large-scale structures, buried in the background turbulence, may not always be detected in the velocity spectra. The clear spectral peaks in Figure 7 suggest that the organizing influence of the excitation is much stronger for the turbulent separation case, as compared to the laminar separation case. Visualization studies of Roos and Kegelman (1986) also support this finding.

Conclusions

The flow over a backward-facing step with nonlaminar separation was investigated experimentally with controlled excitation. Particular emphasis was placed on the instability characteristics of a reattaching shear layer. It was observed that the most dominant structure of such flows was at $St_h = 0.185$, identified as the step mode of instability. The step mode of instability was found to be independent of the separation boundary-layer state.

The previously unexplained phenomenon of concentration of energy at the higher harmonic ($2f$) component of excitation frequency (f), rather than at f itself, was addressed. Energy concentration at the $2f$ component is possible provided that the $2f$ component is a multiple of the step mode of instability. Although the unexcited spectra for both turbulent and transitional separation showed no dominant peak frequency, the downstream growth of u_f with turbulent separation showed that the shear layer had a natural instability frequency at $St_\theta \cong 0.011$.

The high level of turbulence intensity in the separation boundary layer is probably responsible for the inability of a reattaching shear layer with transitional separation to support the downstream growth of a disturbance.

Acknowledgment

We would like to thank the KFUPM for supporting the research in the form of a research assistantship for one of us (A.S.K.). Thanks are also due to Prof. W. H. Stahl of DLR, West Germany, who is currently with our department, for reviewing the manuscript.

References

Bhattarcharjee, S., Scheelke, B. and Troutt, T. R. 1986. Modification of vortex interactions in a reattaching separated flow. *AIAA J.*, **24** (4), 623–629

Brown, G. and Roshko, A. 1974. On density effects and large structure in turbulent mixing layers. *J. Fluid Mech.*, **64**, 775–816

Castro, I. P. and Haque, A. 1987. The structure of a turbulent shear layer bounding a separation region. *J. Fluid Mech.*, **179**, 439–468

Chandrsuda, C. and Bradshaw, P. 1981. Turbulence structure of a reattaching mixing layer. *J. Fluid Mech.*, **110**, 171–194

Eaton, J. K. and Johnston, J. P. 1980. Turbulent flow reattachment: An experimental study of the flow and structure behind a backward-facing step. Report MD-39, Department of Mechanical Engineering, Stanford University, Stanford, CA

Etheridge, D. W. and Kemp, P. H. 1978. Measurements of turbulent flow downstream of a rearward-facing step. *J. Fluid Mech.*, **86** (3), 545–566

Goldstein, M. E. and Hultgren, L. S. 1988. Nonlinear spatial evolution of an externally excited instability wave in a free shear layer. *J. Fluid Mech.*, **197**, 295–330

Hasan, M. A. Z. 1983. The effects of external and self excitations on axisymmetric jet turbulence and noise. Ph.D. dissertation, Mechanical Engineering Dept., University of Houston, Houston, TX

Hasan, M. A. Z. 1992. Flow over a backward-facing step under controlled perturbation: laminar separation. *J. Fluid Mech.*, in press

Husain, Z. D. and Hussain, A. K. M. F. 1983. Natural instability of free shear layers. *AIAA J.*, **21**, 1512–1519

Hussain, A. K. M. F. and Hasan, M. A. Z. 1983. The 'whistler nozzle' phenomenon. *J. Fluid Mech.*, **134**, 431–458

Hussain, A. K. M. F. and Zaman, K. B. M. Q. 1981. The 'preferred mode' of an axisymmetric jet. *J. Fluid Mech.*, **110**, 39–71

Jaroch, M. P. and Fernholz, H. H. 1989. The three-dimensional character of a nominally two-dimensional separated turbulent shear flow. *J. Fluid Mech.*, **205**, 523–552

Khan, A. S. 1990. An experimental study of reattaching flow over a backward facing step with controlled excitation. MS thesis, King Fahd University of Petroleum and Minerals, Dhahran, Saudi Arabia

Kibens, V. 1980. Discrete noise spectrum generated by an acoustically excited jet. *AIAA J.*, **18**, 434–441

Kline, S. J., Cantwell, B. J., and Lilley, G. M. 1982. The 1980/81

AFSOR–HTTM–Stanford Conference in Complex Turbulent Flows. Thermo-Sciences Division, Department of Mechanical Engineering, Stanford University, Stanford, CA

McGuinness, M. 1978. Flow with a separation bubble—steady and unsteady aspects. Ph.D. dissertation, Cambridge University, Cambridge, UK

Moss, W. D. and Baker, S. 1980. Recirculating flows associated with two-dimensional steps. *Aeronaut. Q.*, **31**, 151–172

Roos, F. W. and Kegelman, J. T. 1986. Control of coherent structures in reattaching laminar and turbulent shear layers. *AIAA J.*, **24** (12), 1956–1963

Troutt, T. R., Scheelke, B., and Norman, T. R. 1984. Organized structures in a reattaching separated flow field. *J. Fluid Mech.*, **143**, 413–427

Winant, C. D. and Browand, F. K. 1974. Vortex pairing: The mechanism of turbulent mixing layer growth at moderate Reynolds number. *J. Fluid Mech.*, **63**, 237–255

Zaman, K. B. M. Q. and Hussain, A. K. M. F. 1980. Vortex pairing in a circular jet under controlled excitation. Part I: General response. *J. Fluid Mech.*, **101**, 449–491